

Optical constants of vacuum evaporated polycrystalline cadmium selenide thin films

U. Pal, D. Samanta, S. Ghorai, and A. K. Chaudhuri

Citation: *Journal of Applied Physics* **74**, 6368 (1993); doi: 10.1063/1.355161

View online: <http://dx.doi.org/10.1063/1.355161>

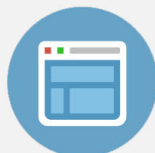
View Table of Contents: <http://scitation.aip.org/content/aip/journal/jap/74/10?ver=pdfcov>

Published by the [AIP Publishing](#)



Re-register for Table of Content Alerts

Create a profile.



Sign up today!



Optical constants of vacuum-evaporated polycrystalline cadmium selenide thin films

U. Pal

Microelectronics Centre, Department of Electronics and ECE, Indian Institute of Technology, Kharagpur-721302, India

D. Samanta and S. Ghorai

Department of Physics, Vidyasagar University, Midnapore-721 102, India

A. K. Chaudhuri

Department of Physics, Indian Institute of Technology, Kharagpur-721 302, India

(Received 19 January 1993; accepted for publication 31 July 1993)

The optical constants (n, K) of vacuum-evaporated polycrystalline CdSe thin films are determined over 900–3100 nm photon wavelengths. Variation of band gap and optical constants with film thickness and substrate temperature is studied. Anomalous variation of refractive index near the band gap is explained by the volume and surface imperfections. Average spin-orbit splitting of valence band (0.32) is estimated for the films deposited on mica substrates. A theoretical plot of refractive index near the band edge is done. The dispersion of refractive index in films is studied by considering a single-oscillator model.

I. INTRODUCTION

Cadmium selenide has been investigated for many years due to its potential use in photoconductive devices and the active elements in photovoltaic solar cells.^{1–3} The suitable direct band gap (1.70 eV) of the material encouraged many workers^{4,5} to study the growth condition of its thin films for use in device fabrication. The growth of wurtzite epitaxial CdSe films on NaCl and mica substrates has been reported by several workers.^{6–8} Optical transmission measurements on wurtzite (hexagonal) and sphalerite (cubic) CdSe epitaxial films deposited on cleaved BaF₂ substrates and on polycrystalline films of CdSe in the ultraviolet region have been reported by Ludeke and Paul⁴ and Sobolev,⁹ respectively. The spin-orbit splitting of the Λ_3 – Λ_1 transition was calculated by Ludeke and Paul⁴ for cubic (0.26 eV) and hexagonal (0.28 eV) phases. A band structure was proposed by them and the optical structure of the compound was interpreted based on the measurements of optical transmission in wurtzite CdSe films. The refractive index of CdSe thin films of different thicknesses deposited on glass and silica substrates has been measured by Dologan¹⁰ from transmittance measurements. Thutupalli and Tomlin¹¹ and El Shazly¹² have prepared CdSe thin films on glass and quartz substrates by vacuum evaporation, and they reported the averaged values of the optical constants obtained from their optical measurements on several films. The variation of optical constants with film thickness for vacuum-evaporated polycrystalline CdSe films has been reported by Shaalan and Müller¹³ from their reflectance and transmittance measurements. Although they studied the variation of optical constants with film thickness for very thin (16–166 nm) CdSe films and presented some interesting results, they could not give a proper explanation of such variations.

In the present work the variation of optical constants (n, K) with film thickness and substrate temperature has been investigated thoroughly for vacuum-evaporated polycrystalline CdSe films deposited on glass substrates. The effect of the nature of the substrates on the variation of optical band gap is studied for the films deposited on glass and mica substrates. The effect of different microstructural parameters such as particle size, RMS strain, etc. on the optical band gap and other optical constants have been studied. The anomalous behavior of the optical constants near the fundamental gap is explained properly.

II. EXPERIMENTS

Polycrystalline cadmium selenide was synthesized from cadmium (99.999%) and selenium (99.999%) in an evacuated ($\sim 10^{-4}$ Pa) quartz ampoule. The details of the synthesis process are reported elsewhere.¹⁴ The final compound was identified to be CdSe (wurtzite) by x-ray powder diffraction. Thin films of CdSe of different thicknesses were deposited on thoroughly cleaned glass and mica substrates at room temperature (303 K) maintaining a rate of deposition of 120 nm/min; however, for the films deposited at different substrate temperatures, the rate of deposition was 150 nm/min. The deposition of the films at different substrate (glass) temperatures was carried out in a suitable apparatus described elsewhere.¹⁵ The composition of the films was estimated by energy-dispersive x-ray analysis (EDX) (canscan series 2DV with link system) analysis. It was observed that the composition of the deposited films varies with film thickness as well as the substrate temperature. The thickness of the films was measured by a Taylor–Hobson form talysurf.

The x-ray-diffraction patterns of the films were recorded by a Phillips (PW 1729) x-ray diffractometer. Par-

ticle size and RMS strain were determined from the line broadening of the x-ray diffraction patterns by variance analysis. It was observed that the particle size increases with the increase of film thickness and substrate temperature. The composition of the films deviated from its stoichiometry with the increase of film thickness. With the increase of substrate temperature stoichiometry improved up to 473 K beyond which it degraded very fast.

The optical absorption and transmittance T of the films were recorded from 400 to 3100 nm wavelength by a Shimadzu (UV-365) double monochromator recording spectrophotometer.

III. RESULTS AND DISCUSSION

It has been observed from the x-ray-diffraction patterns that the CdSe films deposited at room temperature and at elevated temperatures are polycrystalline in nature. The crystallites in the films deposited at room temperature (303 K) are preferentially oriented with the {002} face parallel to the substrate. As the substrate temperature is increased to 473 K and above, the hexagonal {112} peak appears along with the initial hexagonal {002} peak. With the increase of substrate temperature the intensity of the {002} peak increased and hence also the particle size along this orientation. The intensity of the hexagonal {112} peak which appeared at 473 K also increased with the further increase of substrate temperature. The variation of particle size and other microstructural parameters in those two orientations with the variation of substrate temperature T_s has already been reported by the authors.¹⁴

The stoichiometry of the films is found to vary with the variation of film thickness and substrate temperature. With the increase of film thickness, the ratio of Cd and Se (at. %) is increased. The stoichiometry of the films improved up to 473 K substrate temperature for the films deposited on glass substrates, beyond which the ratio of Cd and Se (at. %) exceeded unity sharply. A similar variation of stoichiometry with the variation of film thickness is also observed for the CdSe films deposited on mica substrates.

The transmittance curves of three typical CdSe films of different thickness deposited on glass substrates at room temperature (303 K) are shown in Fig. 1. The transmittance T varied with wavelength λ according to¹⁶

$$T = \frac{16n_\alpha n_g n^2 \exp(-\alpha t)}{R_1^2 + R_2^2 \exp(-2\alpha t) + 2R_1 R_2 \exp(-\alpha t) \cos(4\pi n t / \lambda)} \quad (1)$$

α is the absorption coefficient and n , n_α , and n_g are the refractive indices of the film, air, and substrate respectively. The maxima and minima in the T vs λ plot occur when

$$4\pi n t / \lambda = M\pi, \quad (2)$$

where M represents the order number and t is the thickness of the film. The refractive index n may be computed from the relation^{17,18}

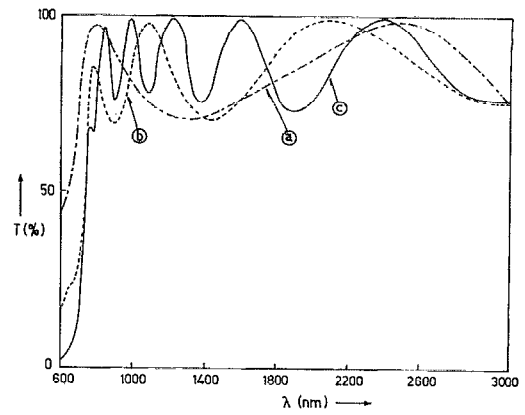


FIG. 1. Transmittance spectrum of (a) 0.18 μm , (b) 0.498 μm , and (c) 0.99 μm CdSe thin films deposited at room temperature (303 K) on the glass substrates.

$$n^2 = (n_\alpha^2 + n_g^2) / 2 + 2n_\alpha n_g T'' + [(n_\alpha^2 + n_g^2 + 4n_\alpha n_g T'')^2 / 4 - n_\alpha^2 n_g^2]^{1/2}, \quad (3)$$

where

$$T'' = (T_{\max} - T_{\min}) / (T_{\max} + T_{\min}).$$

T_{\max} and T_{\min} represent the envelope of the maxima and minima positions of the T vs λ curve (Fig. 1). Exponential variation of T with absorption coefficient α is most probable near the absorption edge, therefore, α may be determined from the relation

$$T = A \exp(-\alpha t), \quad (4)$$

where

$$A = \frac{16n_\alpha n_g (n^2 + K^2)}{[(n_\alpha + n)^2 + K^2][(n_g + n)^2 + K^2]} \quad (5)$$

and K is the extinction coefficient. A is found to be nearly equal to unity at the absorption edge.

The relation between α and incident photon energy $h\nu$ can be written as¹⁹⁻²²

$$\alpha h\nu = C_1 (h\nu - E_g^d)^{1/2}, \quad (6)$$

$$\alpha h\nu = C_2 (h\nu - E_g^i)^2, \quad (7)$$

for allowed direct and indirect transitions, respectively, where C_1 and C_2 are two constants, $\alpha = 4\pi K / \lambda$ is the absorption coefficient, and E_g^d and E_g^i are the direct and indirect band gaps, respectively.

The $(\alpha h\nu)^2$ vs $h\nu$ plots for CdSe films of different thicknesses deposited at room temperature (303 K) on glass substrates are shown in Fig. 2. The graphs of $(\alpha h\nu)^{1/2}$ vs $h\nu$ instead of $(\alpha h\nu)^2$ vs $h\nu$ are found not to lead to straight lines over any part of the optical absorption spectrum, thus supporting the interpretation of direct rather than indirect band gap for all vacuum-deposited films,²³ which is in accordance with the energy-band model of CdSe proposed by Kobayashi *et al.*⁴² The direct band gaps for the films of different thickness are evaluated from

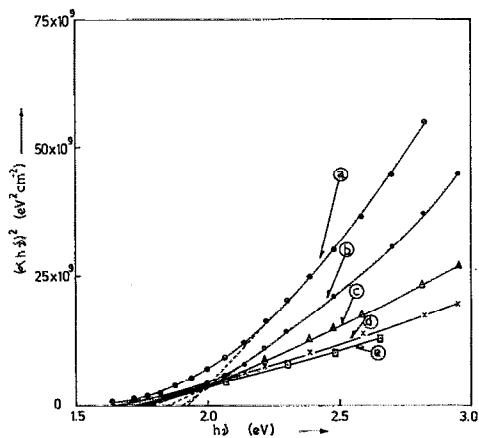


FIG. 2. $(\alpha h\nu)^2$ vs $h\nu$ plots for (a) 0.18 μm , (b) 0.271 μm , (c) 0.42 μm , (d) 0.498 μm , and (e) 0.99 μm CdSe thin films deposited at room temperature (303 K) on the glass substrates.

the x -axis intercepts of $(\alpha h\nu)^2$ vs $h\nu$ plots and it is observed that the band gap decreases with increase of film thickness and also particle size (calculated from x -ray line profile analysis). The direct band gap approaches its bulk value (1.70 eV) with the increase of film thickness. The measured direct-band-gap values for lower film thickness are found to be higher than that for bulk value. Such a variation of band-gap value with film thickness was also reported by Shaalan and Müller.¹³ A comparison of E_g^d with film thickness, particle size, microstrain, and dislocation density is given in Table I. The decrease of E_g^d with increase of film thickness is likely to be attributed to an increase in particle size and a decrease in RMS strain. Although the composition of the films varied with the thickness as estimated by EDX analysis, the excess cadmium in the films is too small to cause other than a very small change in the band gap, by virtue of its effect on composition. Another possibility of such variation of band gap is its particle size dependence. The three-dimensional quantum-size effect, leading to an increase in band gap with a decrease in particle size, is well known for colloidal semiconductor sols where the individual colloidal particles are dispersed in a liquid or glass.²⁴ Several workers^{23,25} have explained the shift of optical band gap (up to 0.5 eV higher) in very thin CdSe films from the single-crystal value in terms of a quantum-size effect. Quantum-size effects on the direct interband transition at the Γ point can

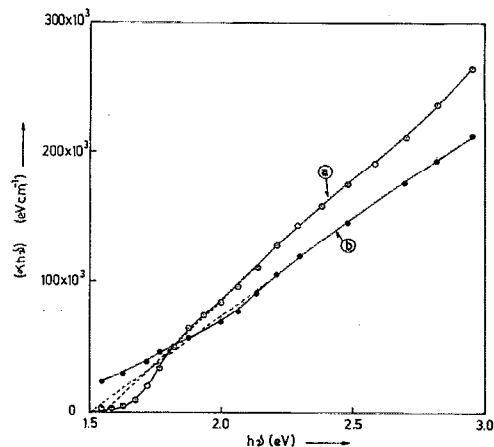


FIG. 3. $\alpha h\nu$ vs $h\nu$ plots for (a) 0.18 μm and (b) 0.271 μm CdSe thin films deposited at room temperature (303 K) on glass substrates.

be easily estimated by using the relation given by Cerdeira *et al.*⁵ For our thinnest film with 28.5 nm particle size the maximum possible shift of band gap due to quantum-size effect could be 72 meV. Therefore, the shift of band gap in the present case is not only due to the smallness of the particles; it is also observed that the curves 2(a) and 2(b) do not show a very good straight-line fit. Because these two films are very thin, the average particle size is observed to be very small, which is shown in Table I. Therefore, there is a possibility of the presence of many very small crystallites in the films which may behave like an amorphous sample and may contribute to the absorption spectrum. Thus, the curvature to the plots of Figs. 2(a) and 2(b) may be due to the influence of the absorption spectrum of the amorphous portion of the film.

For CdSe films deposited on glass substrates a plot of $\alpha h\nu$ vs $h\nu$ gives a better fit (Fig. 3), though the evaluated E_g is lower than the E_g value of the bulk crystal. Such a linear $\alpha h\nu$ vs $h\nu$ dependence has been calculated for transitions between extended states in amorphous semiconductors.²⁶ We believe this deviation from the normal direct-band-gap behavior of CdSe to be due to local strain in the individual crystallites making up the vacuum-evaporated layers.²³ A similar variation of absorption coefficient α with photon energy was also observed by Bazhenov and Krasil'nikova²⁷ for bulk CdSe. They explained such variation by the dislocation absorption mechanism.

TABLE I. Different optical parameters and their comparison with microstructural parameters for CdSe thin films deposited at room temperature (303 K) on the glass substrates.

Film thickness (μm)	Cd/Se (at. %)	Particle size P (nm)	RMS strain $\langle e^2 \rangle^{1/2} \times 10^4$	Dislocation density ρ (10^{14} lines m^{-2})	E_g^d (eV)	Refractive index n at 2.8 μm	S_0 (10^{13} m^{-2})	E_g/S_0 (10^{-14} eV m)
0.180	1.013	28.5	53.88	14.00	1.94	2.24	4.15	9.67
0.271	1.109	37.4	48.21	10.72	1.90	2.25	3.89	9.92
0.420	1.043	59.4	38.17	6.48	1.85	2.27	6.62	7.35
0.498	1.074	66.3	37.71	5.80	1.75	2.28	9.00	6.29
0.990	1.226	91.5	35.70	3.84	1.70	2.30	16.56	4.57

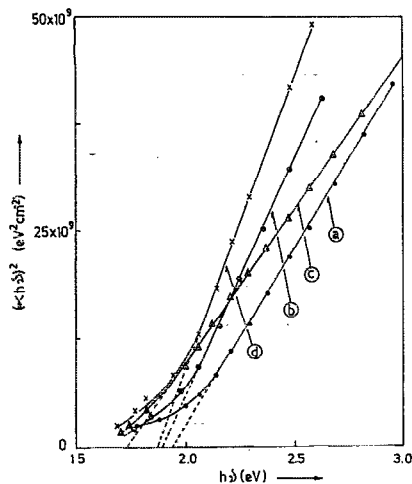


FIG. 4. $(\alpha hv)^2$ vs hv plots for CdSe thin films deposited at (a) 303 K (0.271 μm), (b) 373 K (0.271 μm), (c) 523 K (0.297 μm), and (d) 623 K (0.206 μm) on the glass substrates.

However, the stress field of dislocations may cause a significant strain in the sample.

The $(\alpha hv)^2$ vs hv plots for the CdSe films deposited on glass substrates at different substrate temperatures are shown in Fig. 4. The nature of these curves is very similar to the curves for CdSe films deposited at room temperatures (Fig. 2). As the substrate temperature is increased the stoichiometry is found to improve and the band gap approaches the bulk value from the higher value for $T_s = RT$. Beyond 473 K substrate temperature the stoichiometry is degraded.¹⁴ The effect of such variation of stoichiometry is also reflected in the estimated values of band gaps. The estimated band-gap values are presented in Table II.

The variation of $(\alpha hv)^2$ against hv for the CdSe films of different thicknesses deposited on mica substrates is shown in Fig. 5 (see Table III for other parameters). For each film two straight-line portions are clearly identified and extrapolated to intersect with the x axis at two specific photon energies. In each case two optical transitions are calculated.^{28,29} The band-gap energies for those transitions ($E_g^{d_1}$ and $E_g^{d_2}$) are varied from 1.655 to 1.697 and 1.97 to 2.004 eV, respectively. The optical transitions $E_g^{d_1}$ and $E_g^{d_2}$ of individual CdSe thin evaporated films (on mica) in the range of 0.22 $\mu\text{m} < t < 0.72 \mu\text{m}$ show a variation of their values less than 3%. Similar observations were also

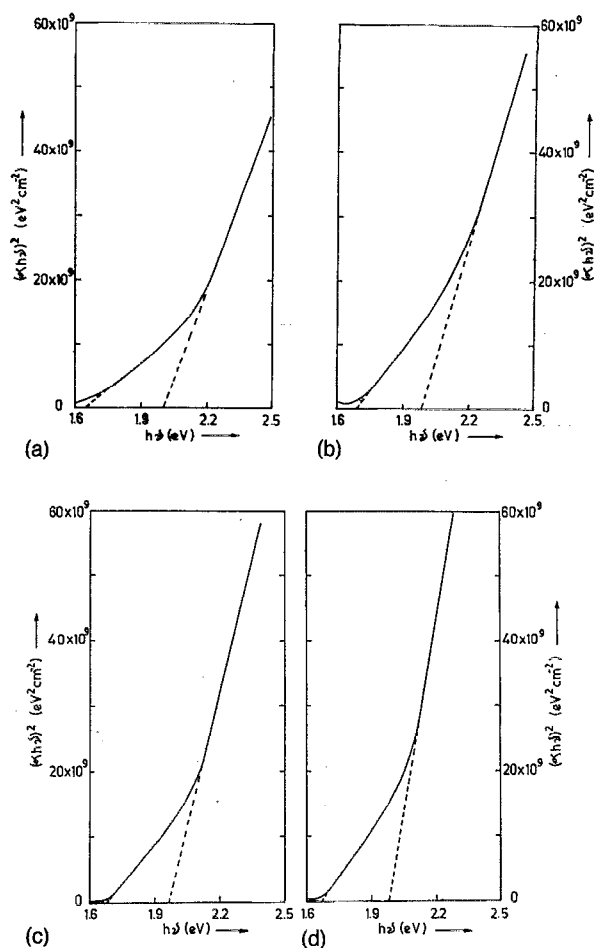


FIG. 5. $(\alpha hv)^2$ vs hv plots for (a) 0.22 μm , (b) 0.24 μm , (c) 0.461 μm , and (d) 0.719 μm CdSe thin films deposited at room temperature (303 K) on mica substrates.

made by Thutupalli and Tomlin¹¹ and Shaalan and Müller¹³ for their vacuum-evaporated CdSe films deposited on glass substrates. The two direct transitions can be attributed to spin-orbit splitting of the valence band which is in agreement with the findings of Cardona, Shaklee, and Pollak,³⁰ but no such splitting could be detected clearly in the absorption spectrum of CdSe film deposited on a glass substrate. Very small humps are seen in the spectrum but from them it is very difficult to resolve another straight portion in a $(\alpha hv)^2$ vs hv plot. Within the limit of experimental accuracy it is not resolved distinctly for the films deposited on a glass substrate. It can be noticed from the

TABLE II. Comparison of different optical parameters with microstructural parameters for CdSe thin films deposited at different substrate temperatures T_s on the glass substrates.

Substrate temp. T_s (K)	Film thickness (μm)	Cd/Se (at. %)	Particle size P (nm)	RMS strain $\langle e^2 \rangle^{1/2} \times 10^4$	Dislocation density ρ (10^{14} lines m^{-2})	E_g^d (eV)	Refractive index n at 2.8 μm	S_o (10^{13} m^{-2})	E_g/S_o (10^{-14} eV m)
303	0.271	1.019	37.4	48.21	14.00	1.90	2.25	3.89	9.92
373	0.271	1.013	46.4	65.40	13.93	1.88	2.24	2.61	11.03
523	0.297	1.017	65.9	43.50	9.26	1.73	2.19	3.75	10.12
623	0.206	1.321	87.0	35.70	4.44	1.87	2.20	4.59	9.48

TABLE III. Comparison of different optical parameters with microstructural parameters for CdSe thin films deposited at room temperatures (303 K) on the mica substrates. S-O indicates "spin orbital."

Film thickness (μm)	Particle size P (nm)	RMS strain $\langle e^2 \rangle^{1/2} \times 10^4$	Dislocation density ρ (10^{14} lines m^{-2})	E^{d_1} (eV)	E^{d_2} (eV)	S-O splitting (eV)	Average S-O splitting (eV)
0.220	26.0	63.45	24.18	1.655	2.004	0.349	0.322
0.240	30.7	53.33	17.26	1.697	1.994	0.297	
0.461	34.8	32.46	3.25	1.624	1.980	0.356	
0.719	66.9	28.72	4.25	1.685	1.970	0.285	

plots of $(\alpha h\nu)^2$ against $h\nu$ that the curves show a nonlinear tailing off to the low energies. This is to be expected for, if additional absorption processes cause the tail at the absorption edge because of transitions from the higher valence level, a similar effect should occur when the transition from the lower of the split valence levels sets in.

Figures 6(a) and 6(b) show the variation of refractive index n and absorption constant K for films of different thickness deposited at room temperature on glass substrates. It is noteworthy that the refractive index n of CdSe films increases with the increase of film thickness. Such a trend of variation is in opposition to that of CdSe films reported by Shaalan and Müller¹³ but a similar variation in

CdTe films has been reported by El Shazly and El Shair.³¹ An anomalous behavior (sometimes a decrease of n) is observed in some of the films at shorter wavelengths. Similar observations have been reported by Manificier and co-workers¹⁶ and Pal *et al.*²² for their Sn_2O_2 and ZnTe films, respectively. Such behavior can be attributed to the strong effect of surface and volume imperfections on a microscopic scale.^{21,32-39} The multiple scattering effects due to the scattering on microscopic inhomogeneities may lead to a serious breakdown of the conventional Kramer-Kronig analysis of reflection and, hence, transmission spectra. The refractive index n and absorption constant K of the films deposited on glass substrates at different temper-

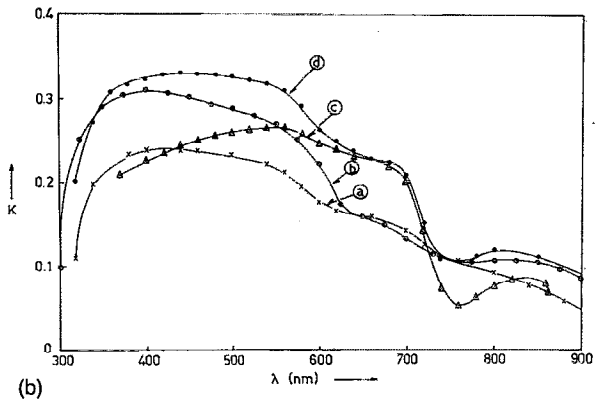
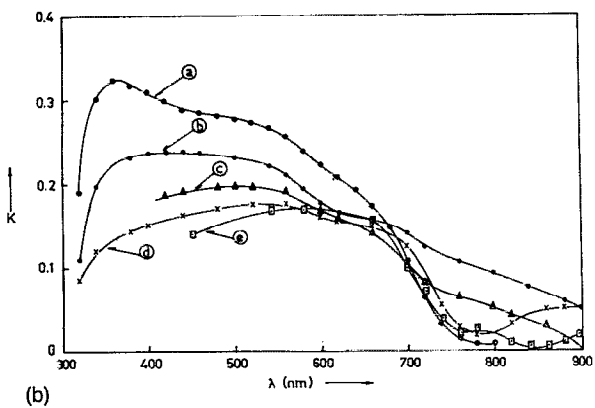
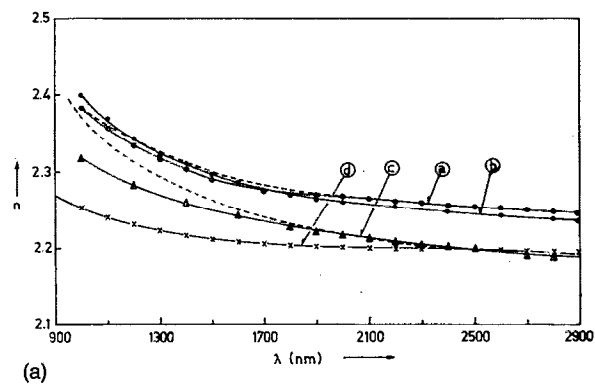
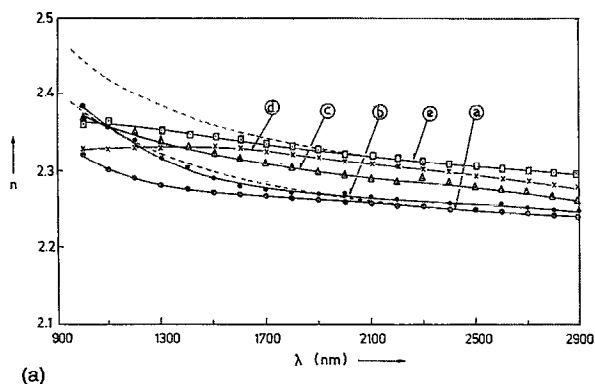


FIG. 6. (a) Variation of refractive index with wavelength for (a) 0.18 μm , (b) 0.271 μm , (c) 0.420 μm , (d) 0.498 μm , and (e) 0.99 μm CdSe thin films deposited at room temperature (303 K) on the glass substrates. (b) Variation of absorption constant K with wavelength for (a) 0.18 μm , (b) 0.271 μm , (c) 0.420 μm , (d) 0.498 μm , and (e) 0.99 μm CdSe thin films deposited at room temperature (303 K) on glass substrates.

FIG. 7. (a) Variation of refractive index n with wavelength for CdSe thin films deposited at (a) 303 K (0.271 μm), (b) 373 K (0.271 μm), (c) 523 K (0.297 μm), and (d) 623 K (0.206 μm) on the glass substrates. (b) Variation of absorption constant K with wavelength for CdSe thin films deposited at (a) 303 K (0.271 μm), (b) 373 K (0.271 μm), (c) 523 K (0.297 μm), and (d) 623 K (0.206 μm) on the glass substrates.

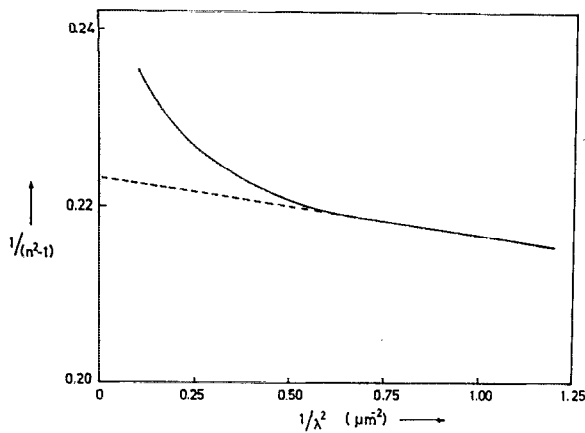


FIG. 8. $1/(n^2-1)$ vs $1/\lambda^2$ plot for a typical CdSe thin film ($0.99 \mu\text{m}$) deposited at room temperature (303 K) on glass substrate.

atures are shown in Figs. 7(a) and 7(b), respectively. The value of refractive index n decreased with increase of substrate temperature. The values of n for room-temperature-deposited films are found to be less than those for the films deposited at higher substrate temperatures. The theoretical plots⁴⁰ of n against λ are shown in Figs. 6(a) and 7(a) for the thinnest ($0.18 \mu\text{m}$) and thickest ($0.99 \mu\text{m}$) CdSe films deposited at room temperature and the film deposited at 623 K substrate temperature, using the experimental parameters and taking the index of refraction at the absorption edge to be $n(0) = 2.68$ in all the cases at their corresponding absorption edges.

The values of K for all the films are very small, which have allowed the light wave to traverse the samples several times and hence produced the interference fringes in the transmission curves.

It is well known from the dispersion theory that in the region of low absorption the index of refraction n is given in a single-oscillator model by the expression

$$n^2 - 1 = \frac{S_0 \lambda_0}{1 - (\lambda_0/\lambda)^2}, \quad (8)$$

where λ_0 is an average oscillator position, and S is an average oscillator strength.⁴¹ The oscillator strength S_0 is derived from the slope of the straight portion of the $1/(n^2-1)$ vs $1/\lambda^2$ curve, while λ_0 follows from the infinite-wavelength intercept. In Fig. 8 a typical $1/(n^2-1)$ vs $1/\lambda^2$ plot for a CdSe film of $0.99 \mu\text{m}$ thickness ($T_s = \text{RT}$) is shown. The average strength of the oscillator and the refractive index dispersion parameter E_0/S_0 have been calculated for all the CdSe films deposited on glass substrates and presented in Tables I and II. The E_0 can be expressed as

$$E_0 = hc/(e\lambda_0), \quad (9)$$

where h is Planck's constant, c is the speed of the light, and e is the electronic charge. It was observed that the strength of the oscillator S_0 increases with the increase of film thickness and substrate temperature.

IV. CONCLUSIONS

The optical transitions in CdSe (wurtzite) films are direct in nature. The direct band gap E_g^d of the films deposited on glass substrates depends critically on the film thickness and substrate temperature. The variation of E_g^d with the variation of film thickness (0.18 – $0.99 \mu\text{m}$) is the cumulative effect of composition, particle size, and strain in the films. Two direct transitions, one at about 1.67 eV and another at about 1.99 eV can be observed for the CdSe films deposited on mica substrates. A spin-orbit splitting of valence band of about 0.32 eV is observed for those hexagonal (wurtzite) films.

The values of the optical constants (n and K) are very sensitive to film thickness and substrate temperature. The abnormal variation of n (either a decrease of n or a flat variation) near the absorption edge can be explained considering the effect of volume and surface imperfections. The nature of variation of n with λ improves with the increase of substrate temperature. The dispersion of the refractive index follows a single-oscillator model.

- ¹ A. Heller, K. G. Chang, and B. Miller, *J. Electrochem. Soc.* **124**, 697 (1977).
- ² D. J. Miller and D. Hanamann, *Sol. Energy Mater.* **4**, 223 (1981).
- ³ R. A. Boudrau and R. D. Rauh, *Sol. Energy Mater.* **7**, 385 (1982).
- ⁴ R. Ludeke and W. Paul, *Phys. Status Solidi* **23**, 413 (1967).
- ⁵ F. Cerdeira, I. Torriani, P. Motisuke, V. Lemos, and F. Decker, *Appl. Phys. A* **46**, 107 (1988).
- ⁶ S. A. Semiletov, *Kristallografiya* **1**, 306 (1956).
- ⁷ L. A. Sergeeva, I. P. Kalinkin, and V. B. Aleskovskii, *Sov. Phys. Cryst.* **10**, 178 (1965).
- ⁸ A. Brunnschweiler, *Nature* **209**, 493 (1966).
- ⁹ V. V. Sobolev, *Sov. Phys. Opt. Spectrosc.* **18**, 456 (1965).
- ¹⁰ V. Dologan, *Rev. Roum. Phys.* **28**, 647 (1983).
- ¹¹ G. M. K. Thutupalli and S. G. Tomlin, *J. Phys. D* **9**, 1639 (1976).
- ¹² A. El Shazly, *Opt. Pura Appl.* **19**, 23 (1986).
- ¹³ M. S. Shaalan and R. Müller, *Sol. Cells* **28**, 185 (1990).
- ¹⁴ U. Pal, D. Samanta, S. Ghorai, B. K. Samantaray, and A. K. Chaudhuri, *J. Phys. D* **25**, 1488 (1992).
- ¹⁵ S. Santhanam, B. K. Samantaray, and A. K. Chaudhuri, *J. Phys. D* **15**, 2531 (1982).
- ¹⁶ J. C. Manificier, J. Gasiot, and J. P. Fillard, *J. Phys. E* **9**, 1002 (1976).
- ¹⁷ A. Mandal, S. Choudhuri, and A. K. Pal, *Appl. Phys. A* **43**, 81 (1987).
- ¹⁸ J. C. Manificier, M. D. Mucia, J. P. Fillard, and E. Vicario, *Thin Solid Films* **14**, 127 (1977).
- ¹⁹ J. Tau, in *Optical Properties of Solids*, edited by F. Abeles (North-Holland, Amsterdam, 1972).
- ²⁰ J. Szezyrbowski and A. Czapl, *Thin Solid Films* **46**, 127 (1977).
- ²¹ E. Khawaja and S. G. Tomlin, *J. Phys. D* **8**, 581 (1975).
- ²² U. Pal, S. Saha, A. K. Chaudhuri, V. V. Rao, and H. D. Banerjee, *J. Phys. D* **22**, 965 (1989).
- ²³ G. Hodes, A.-A. Yaron, F. Decker, and P. Motisuka, *Phys. Rev. B* **36**, 4215 (1987).
- ²⁴ L. E. Brus, *J. Chem. Phys.* **79**, 5566 (1983).
- ²⁵ H. Weller, H. M. Schmidt, U. Koch, A. Fojtik, S. Baral, A. Henglein, W. Kunath, K. S. Weiss, and E. Dieman, *Chem. Phys. Lett.* **124**, 557 (1986).
- ²⁶ R. T. Tripathi, L. L. Moseley, and T. Lukes, *Phys. Status Solidi B* **83**, 197 (1977).
- ²⁷ A. V. Bazhenov and L. L. Krasil'nikova, *Sov. Phys. Solid State* **26**, 356 (1984).
- ²⁸ T. S. Moss, *Optical Properties of Semiconductors* (Butterworths, London, 1961).
- ²⁹ T. S. Moss, G. J. Burrell, and B. Ellis, *Semiconductor Optoelectronics* (Butterworths, London, 1973).
- ³⁰ M. Cardona, K. L. Shaklee, and F. H. Pollak, *Phys. Rev.* **154**, 696 (1967).

- ³¹A. A. El Shazly and H. T. El Shair, *Thin Solid Films* **78**, 287 (1981).
³²J. M. Pawlikowskii, *Thin Solid Films* **127**, 39 (1985).
³³H. E. Bennett and J. M. Bennett, *Thin Solid Films* **4**, 3 (1967).
³⁴P. Rouard and A. Messen, *Prog. Opt.* **15**, 79 (1977).
³⁵J. Casset, *C. R. Acad. Sci. Paris B* **263**, 299 (1966).
³⁶D. W. Berreman, *Phys. Rev.* **163**, 855 (1967).
³⁷M. E. Bennet and J. O. Poters, *J. Opt. Soc. Am.* **51**, 123 (1969).
³⁸D. Beaglehole and O. Hunderi, *Phys. Rev. B* **2**, 309 (1970).
³⁹D. G. Thomas, *J. Phys. Chem. Solids* **15**, 86 (1960).
⁴⁰B. Jensen and A. Torabi, *J. Appl. Phys.* **54**, 2030 (1983).
⁴¹M. Di Domenico and S. H. Wemple, *J. Appl. Phys.* **40**, 720 (1969).
⁴²A. Kobayashi, O. F. Sankey, S. M. Volz, and J. D. Dow, *Phys. Rev. B* **28**, 935 (1983).